Published in final edited form as:
Nanoscale. 2010 September ; 2(9): 1715–1722. doi:10.1039/c0nr00303d.

Design and Characterization of Optical Nano Rulers of Single Nanoparticles Using Optical Microscopy and Spectroscopy

Prakash D. Nallathamby, **Tao Huang**, and **Xiao-Hong Nancy Xu***
Department of Chemistry and Biochemistry, Old Dominion University, Norfolk, VA 23529

Abstract

Current conventional imaging methods cannot determine sizes of single nanoparticles (NPs) in solution and living organisms at nanometer scale, which limits the applications of NPs. In this study, we developed new imaging calibration approaches to characterize the sizes of single Ag NPs in solution at nanometer resolution by measuring their size-dependent scattering localized-surface-plasmon-resonance (LSPR) spectra and scattering intensity using dark-field optical microscopy and spectroscopy (DFOMS). We synthesized nearly spherical shape Ag NPs, ranging from 2 to 110 nm in diameter, and characterized the sizes of single NPs using high-resolution transmission electron microscopy, and the LSPR spectra and scattering intensity of single NPs using DFOMS. We constructed calibration curves of the peak wavelength (λ_{max}) of LSPR spectra or scattering intensity of single NPs versus their sizes. These calibration curves allow us to determine the sizes of single NPs at 1 nm resolution by measuring the LSPR spectra or scattering intensity of single NPs using DFOMS. These new approaches enable us to create optical nano rulers (calibration curves) of single Ag NPs for simultaneously imaging and measuring sizes of multiple single NPs in solution in real-time at nanometer resolution using optical microscopy. One can now use these new imaging calibration approaches to study and characterize single NPs in solution and living organisms in real time for a wide variety of applications.

Keywords

nanophotonics; noble metal nanoparticles; single nanoparticle optics; single nanoparticle imaging; plasmonic spectroscopy

Introduction

Noble metal nanoparticles (NPs) (e.g., Ag, Au) exhibit size-dependent optical, electronic and catalytic properties,[1–8] emphasizing the importance of characterization of the sizes of single NPs *in situ* and in real-time.[9–13] Up to date, primary means to determine the sizes of single NPs is electron microscopy (EM), such as transmission electron microscopy (TEM) and scanning electron microscopy (SEM). However, EMs have to be operated under high vacuum, which is not suitable for imaging single NPs in solution and living organisms. Atomic force microscopy (AFM) and scanning tunning microscopy (STM) have been used to image the size and shape of noble metal NPs in solution,[7, 14] but they are unable to image free diffusion of single NPs in solution and in living organisms. The slow speed of AFM and STM prohibits their use for high-througput analysis and real-time imaging of large number of single NPs simulatenousy. These limitations demand the development of new imaging tools to

*To whom correspondence should be addressed: xhxu@odu.edu; www.odu.edu/sci/xu/xu.htm; Tel/fax: (757) 683-5698.

characterize sizes of mutiple single NPs in solution and in living organisms rapidly and simultaneously.

Studies have showed that noble metal (e.g., Ag) NPs possess exceptionally high quantum yield of Rayleigh scattering that are orders of magnitude higher than fluorophors (e.g., R6G),[4, 15, 16] and they can be directly imaged and characterized using dark-field optical microscopy and spectroscopy (DFOMS).[9, 10, 17–20] For example, DFOMS has been used to image multiple single NPs in solution and in living organisms in real-time at millisecond temporal resolution simultaneously.[9, 10, 16–19, 21–23] Unlike fluorophors and semiconductor quantum dots (QDs), these noble metal NPs show superior photostability (non-photobleaching and non-blinking), allowing them to serve as photostable nanophotonic optical probes for sensing and imaging single molecules and dynamics events of interest in single living cells and living embryos for desired period of time.[9, 10, 17, 18, 24] However, the optical diffraction limit prohibits the use of optical microscopy to determine and measure the sizes of NPs at the nanometer resolution.

According to Mie theory,[5] the localized-surface-plasmon-resonance (LSPR) spectra and scattering intensity of single spherical NPs depend upon the sizes, shapes and surrounding environments (e.g., dielectric constant of embedded medium) of single NPs. Several studies have used simulation to systematically demonstrate the size- and shape- dependent optical properties of single noble metal NPs.[1, 2, 25, 26] With recent advance in nanofrication and wet chemical synthesis, it is possible to prepare desired shapes and sizes of NPs.[1, 7, 8, 14] These advances enable the experimental observation of size- and shape- dependent optical properties of single NPs.[1, 23]

These properties suggest the possibility of using LSPR spectra or scattering intensity of single spherical Ag NPs to determine the sizes of single NPs at the nanometer scale using DFOMS, if one can keep the shape and surrounding environments of single NPs in constant and determine the calibration curves of the peak-wavelength (λ_{max}) of LSPR spectra or scattering intensity of single NPs with the sizes of single NPs.

In our previous studies, we have demonstrated the possibility of using size-dependent optical properties of single NPs to determine the sizes of single spherical Ag and Au NPs and to measure the size transformation of membrane pores of single living cells in real time.[21–23, 27] However, experimental calibration approaches for single Ag NPs from 2–110 nm using LSPR spectra and scattering intensity of single NPs have not yet been reported previously.

In this study, we demonstrate the possibility of using size-dependent LSPR spectra and scattering intensity of single Ag NPs to create optical nano rulers (calibration curves) and use them to measure sizes of single Ag NPs at nanometer scale in real time using DFOMS. Molecular rulers and plasmon rulers have been described as rulers for determining distances between molecules or NPs.[28, 29] In this study, we define our optical nano rulers as a measure for determining sizes of single NPs using size-dependent LSPR spectra or scattering intensity of single NPs.

Results and Discussion

Synthesis and Characterization of Sizes and Shapes of Single Ag NPs using HRTEM

We have synthesized four groups of Ag NPs with various sizes, as described in Experimental Section, and characterized their sizes and shapes using HR-TEM. The results in Figures 1A-D show the sizes of Ag NPs with average diameters of 3.1 ± 0.6, 13.4 ± 5.8, 46.4 ± 6.1, and 91.1 ± 7.6 nm, respectively. The shapes of Ag NPs in Figures 1A-B are nearly spherical, while those in Figures 1C-D are less spherical with some being polygon with sharp edges and some with aspect ratio slightly larger than one. The diameters of single NPs in Figures 1C-D are

calculated by averaging the lengths of NPs in both dimensions. Notably, we did not observe any NPs with irregular shapes (e.g., rod or triangle). Overall, the shapes of NPs in all four NP solutions are nearly spherical, as shown in Figures 1A-D.

We characterized the plasmonic absorption and scattering of bulk Ag NP solution using UV-vis absorption spectroscopy. The results in Figure 2A show the peak wavelength of absorption spectra of NP solutions with its full-width-of-half-maximum (FWHM) are 390 nm (FWHM = 62 nm), 393 nm (FWHM = 65 nm), 408 nm (FWHM = 82 nm), and 440 nm (FWHM = 152 nm) with a shoulder peak at 384 nm, for 3.1 ± 0.6, 13.4 ± 5.8, 46.4 ± 6.1, and 91.1 ± 7.6 nm NP solutions, respectively. The shoulder peak in Figure 2A-d is likely attributable to the in-plane quadrupole resonance of NPs, which is generated by transverse collective oscillation of the surface electrons between the edges of the NPs, as described previously by theoretical simulation.[2, 7, 25] Note that some NPs in Figure 1D are polygon with sharp edges. The photos of the NP solutions in Figure 2B show the transparent light yellow, yellow, dark-yellow, and cloudy silver colors, respectively.

The results in Figure 2 illustrate the size-dependent plasmonic absorption and scattering of Ag NPs in solution, showing the shorter peak-wavelength of absorption spectra for the smaller NPs, which agrees with those described in literature.[1–4] The FWHM of the absorption spectra reflects the size distribution of NPs in each solution, suggesting that the smaller NPs (Figures 2A and B) are much more uniform in size than the larger NPs (Figures 2C and D), which agrees with results shown in Figure 1 and as those we reported previously.[3, 4, 10, 15]

Imaging and Characterization of LSPR Spectra of Single Ag NPs using DFOMS

We acquired optical images and LSPR spectra of single Ag NPs for each NP solution using DFOMS. Our dark-field optical microscope offers the depth of field (focus) of 190 nm, as described in Experimental Section. Notably, the illumination of dark-field optical microscopy focuses on the sample and then diverts from the microscopic objective. Thereby, it provides a dark background, and only scattering intensity of specimens (e.g., NPs) on the focal plane is collected by the microscope objective and recorded by detectors (e.g., CCD). Therefore, the LSPR spectra and intensity of single NPs acquired by DFOMS are the results of the scattering of NPs, but not absorption of NPs.

The results in Figures 3A-D show the representative optical images (Figure 3a) and LSPR spectra of single NPs (Figure 3b), and distribution of λ_{max} of LSPR spectra of more than 300 of single NPs (Figure 3c), for 3.1 ± 0.6, 13.4 ± 5.8, 46.4 ± 6.1, and 91.1 ± 7.6 nm NP solution, respectively. For each NP solution, more than 20 images, similar to those in Figure 3a, are acquired and the LSPR spectra of more than 300 of single NPs are characterized, which ensures that the distribution of λ_{max} of LSPR spectra of single NPs represents the bulk NP solution at the single-NP resolution. We define the colors of single NPs using the λ_{max} of their LSPR spectra. For example, violet, blue, green, yellow, and red NPs are the single NPs with the λ_{max} of the LSPR spectra at 436–450 nm, 451–484 nm, 492–560 nm, 564–580 nm, and 590–717 nm, respectively.

Representative optical image of single NPs in Figure 3A-a show single violet and blue NPs for 3.1 ± 0.6 nm Ag NP solution. Representative LSPR spectra of single NPs in Figure 3A-b show their λ_{max} at (i) 453 and (ii) 456 nm. The histogram of distribution of λ_{max} of the LSPR spectra of more than 300 single NPs in Figure 3A-c illustrates that the λ_{max} ranges from 436 to 484 nm with an average at 455 ± 10 nm, and the solution contains 40% of violet NPs and 60% of blue NPs.

Representative optical image of single NPs in Figure 3B-a show single violet, blue, green, yellow, and red NPs, and representative LSPR spectra of single NPs in Figure 3B-b show their

λ_{max} at (i) 468, (ii) 475, (iii) 488, and (iv) 456 nm, for 13.4 ± 5.8 nm Ag NP solution. The histogram of distribution of λ_{max} of the LSPR spectra of single NPs in Figure 3B-c shows that their λ_{max} ranges from 439 to 596 nm with an average at 475 ± 32 nm, and the solution consists of 77% of blue, 19% of green, 1% of yellow, and 3% of red NPs.

We observed single blue, green, yellow, and red NPs in Figure 3C-a, and the λ_{max} of representative LSPR spectra of single NPs at (i) 482, (ii) 502, (iii) 533, and (iv) 554 nm in Figure 3C-b for 46.4 ± 6.1 nm Ag NP solution. The distribution of λ_{max} of LSPR spectra of single NPs ranges from 460 to 595 nm with an average of 512 ± 32 nm, as shown in Figure 3C-c. The Ag NP solution has 1% of blue, 60% of green, 3% of yellow, and 6% of red NPs.

We found single green, yellow and red NPs in Figure 3D-a, and the λ_{max} of representative LSPR spectra of single NPs at (i) 552, (ii) 557, (iii) 558, (iv) 574, and (v) 644 nm, in Figure 3D-b, for 91.1 ± 7.6 nm Ag NP solution. The distribution of λ_{max} of LSPR spectra of single NPs ranges from 543 to 650 nm with an average of 561 ± 25 nm, as shown in Figure 3D-c. The Ag NP solution has 68% of green, 15% of yellow and 17% of red NP.

Taken together, optical images and histograms of λ_{max} of LSPR spectra of single Ag NPs in Figure 3 show size-dependent LSPR spectra with various λ_{max} (colors) and illustrate the red-shift of LSPR spectra as the size of the NPs increases. Representative LSPR spectra of single NPs show the narrower distribution of λ_{max} and smaller FWHM for smaller NPs in Figures 3A-B, and wider distribution of λ_{max} with larger FWHM for lager NPs in Figures 3C-D. The results show more uniform sizes and shapes of NPs in Figures 3A and B and less uniform sizes and shapes of NPs in Figures 3C and D, which agrees with the sizes that are characterized using HRTEM in Figure 1.

It is worth noting that the LSPR spectra in Figure 3 are acquired from scattering of individual NPs, while the UV-vis absorption spectra in Figure 2A are obtained from absorption and scattering of bulk NP solution (ensemble measurements). Therefore, the UV-vis absorption spectra of bulk NP solutions in Figure 2 differ from LSPR spectra of single NPs (Figure 3), for each given solution.

Characterization of Scattering Intensity of Single Ag NPs using DFOMS

Using the same approaches, we acquired optical images of single Ag NPs and measured Rayleigh scattering intensity of single Ag NPs for each NP solution using DFOMS. The results in Figures 4A-D show the representative optical images of single NPs (Figure 4a) and distribution of scattering intensity of more than 300 of single NPs (Figure 4b) for 3.1 ± 0.6, 13.4 ± 5.8, 46.4 ± 6.1, and 91.1 ± 7.6 nm Ag NP solution, respectively.

For each NP solution, we acquired more than 20 images, similar to the one in Figure 4a, and measured the scattering intensity of more than 300 of single NPs. The scattering intensity of individual NPs was measured by subtracting the average background intensity of individual background areas (20x20 pixel) in the absence of NPs from the integrated intensity of a single NP in the detection area (20x20 pixel), as illustrated in Figure 4B-a. Each histogram of the scattering intensity of single NPs for more than 300 NPs in Figure 4b illustrates the distribution of scattering intensity of single NPs for each NP solution. This approach provides sufficient statistics, which allows the distribution of scattering intensity of single NPs to represent the bulk NP solutions at the single-NP resolution.

The dark-field optical images and histograms of the scattering intensity of single Ag NPs (Figures 4A-D) show that intensity of single NPs ranges from 20 to 600 analog-to-digital counts (ADC) with the average of 430 ± 199 ADC for 3.1 ± 0.6 nm Ag NPs in Figure 4A, 300 to 1050 ADC with the average of 685 ± 202 ADC for 13.1 ± 5.8 nm NPs in Figure 4B, 5.6×10^3 to

2.1×10^5 ADC with the average of $(1.3 \pm 0.4) \times10^4$ ADC for 46.4 ± 6.1 nm NPs in Figure 4C, and 6×10^4 to 1×10^6 ADC with the average of $(7.8 \pm 0.96) \times10^5$ ADC for 91.1 ± 7.6 nm Ag NPs in Figure 4D.

Taken together, the results in Figure 4 show that scattering intensity of single Ag NPs highly depends upon their sizes, which agrees with those described in literature.[2, 3, 5] Optical images of single NPs acquired by a high sensitivity CCD camera, and histograms of scattering intensity of single NPs in Figure 4 show that smaller Ag NPs exhibit lower scattering intensity, and the scattering intensity of single NPs increases as the size of NPs increases. The results suggest the possibility of using scattering intensity of single Ag NPs to generate optical nano rulers for characterizing the sizes of single Ag NPs using dark-field optical microscopy.

Creation of Optical Nano Rulers by Correlating LSPR Spectra of Single Ag NPs with their Sizes

We correlate each histogram of the λ_{max} of LSPR spectra of single NPs determined by DFOMS in Figure 3c with the size distribution of single NPs measured by HRTEM in Figure 1b for each NP solution, respectively. The results in Figure 5 show a linear correlation of the λ_{max} of LSPR spectra of single NPs with their sizes, allowing us to create a calibration curve of the λ_{max} of LSPR spectra of single NPs versus the sizes of single NPs for each Ag NP solution, 3.1 ± 0.6, 13.4 ± 5.8, 46.4 ± 6.1, and 91.1 ± 7.6 nm Ag NPs, respectively.

Linear plots were observed for the smaller NPs (2–10 nm and 9–31 nm) in Figures 5A and B, and larger NPs (37–62 nm; 86–104 nm) in Figures 5C and D. Interestingly, two linear curves are observed for the NPs with average diameters of 91.1 ± 7.6 nm (86–104 nm), suggesting the high dependence of the λ_{max} of LSPR spectra of single NPs on their shapes. Notably, the largest NPs are less spherical and contain some polygon NPs, as shown in Figure 1D. The calibration curves allow us to generate optical nano rulers (calibration curves) for imaging and measuring the sizes of NPs using DFOMS. For example, one can measure the LSPR spectra of single NPs in each NP solution using DFOMS, and use the λ_{max} of LSPR spectra of single NPs to determine the sizes of single NPs via the calibration curves in Figure 5.

There are some overlaps for the NPs in Figures 5B and C, which may be attributed to the different dielectric constants of solutions and various shapes of NPs. Note that a much higher concentration of sodium citrate was used to synthesize larger NPs, which may lead to the different dielectric constants on the surface of NPs. The results show the high dependence of the λ_{max} of LSPR spectra of single NPs on their surrounding environments (e.g., surface adsorbates, dielectric constant of embedded medium), suggesting the importance of calibration approaches for each NP solution.

Constructions of Optical Nano Rulers by Correlating Scattering Intensity of Single Ag NPs with their Sizes

We also correlate each histogram of the scattering intensity of single NPs determined by DFOMS in Figure 4b with the size distribution of single NPs measured by HRTEM in Figure 1b, for each NP solution. The results in Figure 6 show a linear correlation of the scattering intensity of single NPs with their sizes, which enables us to generate a calibration curve of the scattering intensity of single NPs versus the sizes of single NPs for each Ag NP solution, 3.1 ± 0.6, 13.4 ± 5.8, 46.4 ± 6.1, and 91.1 ± 7.6 nm Ag NPs, respectively. Notably, linear calibration curves are observed for all four NP solutions.

Unlike observed in Figure 5D, a linear calibration curve is found for the largest NPs (91.1 ± 7.6 nm) in Figure 6D, suggesting that scattering intensity of single NPs is less sensitive to their shapes than the LSPR spectra. Notably, no overlap is observed among NP solutions,

demonstrating that scattering intensity of single NPs is less sensitive to their surrounding environments.

Each calibration curve in Figure 6 allows us to generate optical nano rulers for characterization of the sizes of single NPs using DFOMS. For instance, one can measure the scattering intensity of single NPs in each NP solution using DFOMS, and use the scattering intensity of single NPs to determine the sizes of single NPs via the calibration curves in Figure 6.

Taken together, we have constructed the calibration curves of the λ_{max} of LSPR spectra or scattering intensity of single Ag NPs measured by DFOMS versus the sizes of single NPs determined by HRTEM for each NP solution. The results are summarized in Table 1. The linear calibration curves enable us to create optical nano rulers to measure the sizes of single NPs in solution by characterizing the LSPR spectra or scattering intensity of single NPs using DFOMS.

This new imaging calibration approach possesses the superior characteristics of optical microscopy for probing dynamic events of interest *in situ* and *in vivo*, as well as overcomes its optical diffraction limit, enabling the characterization of single NPs in solution at nanometer scale in real time. Notably, the noble metal NPs show superior photostability (non-photobleaching and non-blinking), allowing them to serve as optical probes for study of dynamic events of interest in solution and living organisms for desired period of time.[9, 10, 18]

One potential limitation of these calibration approaches is that one needs to construct the optical nano rulers for each new NP solution and the shapes of NPs in each solution need to be essentially identical, in order to achieve high accuracy and precision of measurements of sizes of NPs.

Experimental Section

Reagents and Supplies

Sodium citrate dihydrate (99%, Sigma-Aldrich), silver perchlorate monohydrate (99%, Alfa Aesar), silver nitrate (>99%, Sigma-Aldrich), sodium borohydride (98%, Sigma-Aldrich), polyvinylpyrrolidone (PVP) (>99%, Sigma-Aldrich), and hydrogen peroxide (30% w/v, Sigma-Aldrich) were purchased and used as received. All solutions were prepared using nanopure deionized (DI) water (18 MΩ, Barnstead). Glassware was cleaned using aqua regia, rinsed thoroughly with nanopure water, and dried prior to the use for synthesis.

Synthesis and Characterization of Single Ag NPs

Ag NPs with average diameters of 3.1 ± 0.6 nm (1.7–6 nm) were synthesized as we described previously.[18] Briefly, $NaBH_4$ (150 μL, 100 mM) was added into a stirring mixture (42.3 mL) of silver nitrate (0.11 mM), sodium citrate (1.91 mM), PVP (0.052 mM), and hydrogen peroxide (25.0 mM) that were freshly prepared using nanopure water. The solution was stirred at room temperature for another 3 h, filtered using 0.2 μm membrane filters and stored in the dark at 4°C until use.

Ag NPs with average diameters of 13.4 ± 5.8 nm (5–45 nm) were prepared by rapidly adding ice-cold $AgClO_4$ (2.5 mL of 10 mM) into a stirring ice-cold mixture (247.5 mL) of sodium citrate (3 mM) and $NaBH_4$ (10 mM), as we described previously.[9, 10] The solution was stirring at room temperature for 4 h, filtered using 0.2 μm filters and washed twice with nanopure water using ultracentrifugation at 15,000 rcf (relative centrifugal force) to prepare stable and purified Ag NPs. The washed Ag NPs were resuspended in nanopure water and stored in the dark at 4° C until use.

We synthesized Ag NPs with average diameters of (46.4 ± 6.1) (35–66 nm) and (91.1 ± 7.6) nm (70–110 nm) by adding sodium citrate (10 mL, 34 mM) into a refluxing (100°C) aqueous solution of 1.06 or 3.98 mM $AgNO_3$ (500 mL), respectively. The mixtures were stirred at 325 rpm for 45 or 35 min, respectively, and cooled to room temperature. We added additional 2.5 mM sodium citrate, as a stabilizer, into (91.1 ± 7.6) nm Ag NPs solution. Both solutions were filtered using 0.2 μm filters and stored in the dark at 4°C until use.

Ag NPs in each solution were characterized using high resolution transmission electron microscopy (HRTEM, FEI Tecnai G2 F30, FEG at 300kV), UV-vis spectroscopy (Hitachi U-2010), and dark-field optical microscopy and spectroscopy (DFOMS) (also named as SNOMS by us). Design and construction of our DFOMS has been fully described in our previous studies for real-time imaging and spectroscopic characterization of single NPs in solutions,[9, 10, 30] in single living cells[17, 18, 21–24, 31] and in single zebrafish embryos,[9, 10, 30] and for single molecule detection.[12, 18, 32] These Ag NPs are stable (non-aggregated) in nanopure DI water for months, as we reported previously.[9, 10, 17, 18, 24]

Imaging and Characterization of Scattering LSPR spectra and Intensity of Single Ag NPs

We acquired optical images and LSPR spectra of single Ag NPs in a microchamber using our DFOMS, as we described previously.[21–23, 31, 32] In this study, we used, Nuance Multispectral Imaging Systems (CRI) and other detectors (Roper Scientific EMCCD and 5MHz Micromax CCD camera, and color digital camera), to acquire optical images, LSPR spectra and scattering intensity of single Ag NPs. The scattering intensity of single Ag NPs was acquired using DFOMS equipped with a CCD camera (5 MHZ Micromax or EMCCD) with exposure time of 100 ms.

Our dark-field optical microscope was equipped with a dark-field condenser (Oil 1.43-1.20, Nikon), a microscope illuminator (Halogen lamp, 100W), and a 100x objective (Nikon Plan fluor 100x oil, iris, SL. N.A. 0.5–1.3, W.D. 0.20 mm), offering the depth of field (focus) of 190 nm. Unlike bright-field microscopy, the illumination of dark-field optical microscopy does not pass through the sample, but is focused onto the sample and then diverted from the objective. This design offers a dark background, and only scattering intensity of objects (e.g., NPs) on the focal plane is collected by the microscope objective and recorded by detectors (e.g., CCD). Therefore, the LSPR spectra and intensity of single NPs acquired by DFOMS are resulted from the scattering of NPs, but not absorption of NPs

Construction of Calibration Curves and Optical Nano Rulers

We characterized sizes, LSPR spectra and scattering intensity of more than a hundred of single NPs for each measurement of every NP solution using HRTEM and DFOMS, respectively. A minimal of three measurements was carried out for each NP solution. Therefore, a minimal of 300 single NPs for each NP solution was studied to gain sufficient statistics to characterize the distribution of sizes and size-dependent LSPR spectra and scattering intensity of single NPs that represent the bulk NP solutions at the single-NP resolution. The percentages of violet, blue, green, yellow, and red NPs were determined from the histograms of the λ_{max} of the LSPR spectra of single Ag NPs for each NP solution.

The scattering intensity of individual NPs within a 20x20 pixel area and average background intensity of several detection areas with the same size of detection volume (20x20 pixel) in the absence of NPs were measured, as we described previously.[10, 18] We then subtracted the average background intensity of individual background areas from the integrated intensity of single NPs, to obtain the scattering intensity of single NPs.

We correlated histogram of the distribution of size-dependent peak-wavelength (λ_{max}) of LSPR spectra or scattering intensity of single Ag NPs acquired by DFOMS, with the size distribution (histogram) of single NPs measured by HRTEM for each NP solution. The correlations enable us to create calibration curves and generate optical nano rulers of LSPR spectra or scattering intensity of single Ag NPs versus the sizes of single NPs. These calibration curves (optical nano rulers) allow us to image and characterize the sizes of single Ag NPs by measuring the LSPR spectra or scattering intensity of single Ag NPs using DFOMS.

Summary

In summary, we have developed new imaging calibration approaches to create optical nano rulers (calibration curves) by correlating the histogram of the distribution of λ_{max} of the LSPR spectra or scattering intensities of single Ag NPs with that of the diameters of single NPs for spherical shape Ag NPs dispersed in nanopure DI water. The results show the linear calibration curves of the λ_{max} of the LSPR spectra or scattering intensities of single Ag NPs versus the sizes of single NPs, enabling us to characterize single NPs at nanometer scale in real time using DFOMS. We found that the λ_{max} of the LSPR spectra of single NPs highly depends upon their shapes and surrounding environments. In contrast, the scattering intensities of single NPs are less sensitive to the shapes and surrounding environments of NPs. By combining both calibration curves, we accurately determined the sizes of single NPs in solution. This new imaging calibration approach possesses the superior characteristics of optical microscopy for probing dynamic events of interest *in situ* and *in vivo*, as well as overcomes its optical diffraction limit, allowing simultaneously image and identify sizes of multiple single NPs in solution and living organisms in real-time for a wide variety of applications.

Acknowledgments

This work is supported in part by NSF (NIRT: BES 0507036) and NIH (R01 GM076440). Nallathamby is grateful for the support of Dominion Scholar Fellowship. We thank CharFac of U. of Minnesota (a NNIN site funded by NSF) for their assistance to characterize Ag nanoparticles using HRTEM.

References

1. Pastoriza-Santos I, Liz-Marzan LM. J Mat Chem 2008;18:1724.
2. Kelly KL, Coronado E, Zhao LL, Schatz GC. J Phys Chem B 2003;107:668–677.
3. Bohren, CF.; Huffman, DR. Absorption and Scattering of Light by Small Particles. Wiley; 1983.
4. Kreibig, U.; Vollme, M. Optical Properties of Metal Clusters. Springer; 1995.
5. Mie G. Ann Phys 1908;25:377.
6. Ozbay E. Science 2006;311:189. [PubMed: 16410515]
7. Song Y, Nallathamby PD, Huang T, Elsayled-Ali H, Xu XHN. J Phys Chem C 2010;114:74.
8. Xia Y, Xiong Y, Lim B, Skrabalak SE. Angew Chem Int Ed Engl 2009;48:60. [PubMed: 19053095]
9. Lee KJ, Nallathamby PD, Browning LM, Osgood CJ, Xu XHN. ACS Nano 2007;1:133. [PubMed: 19122772]
10. Nallathamby PD, Lee KJ, Xu XHN. ACS Nano 2008;2:1371. [PubMed: 19206304]
11. Shen Y, Friend C, Jiang Y, Jakubczyk D, Swiatkiewicz J, Prasad P. J Phys Chem B 2000;104:7577.
12. Xu, X-HN.; Song, Y.; Nallathamby, PD. Probing Membrane Transport of Single Live Cells Using Single Molecule Detection and Single Nanoparticle Assay. Xu, X-HN., editor. New Jersey: 2007.
13. Murphy CJ, Gole AM, Stone JW, Sisco PN, Alkilany AM, Goldsmith EC, Baxter SC. Acc Chem Res 2008;41:1721. [PubMed: 18712884]
14. Haes AJ, Zhao J, Zou S, Own CS, Marks LD, Schatz GC, Van Duyne RP. J Phys Chem B 2005;109:11158. [PubMed: 16852361]
15. Jain PK, Huang X, El-Sayed IH, El-Sayed MA. Acc Chem Res 2008;41:1578–1586. [PubMed: 18447366]

16. Yguerabide J, Yguerabide EE. Anal Biochem 1998;262:157. [PubMed: 9750129]
17. Huang T, Nallathamby PD, Gillet D, Xu XHN. Anal Chem 2007;79:7708. [PubMed: 17867652]
18. Huang T, Nallathamby PD, Xu XHN. J Am Chem Soc 2008;130:17095. [PubMed: 19053435]
19. Schultz S, Smith DR, Mock JJ, Schultz DA. Proc Natl Acad Sci U S A 2000;97:996. [PubMed: 10655473]
20. Chan GH, Zhao J, Schatz GC, Van Duyne RP. J Phys Chem C 2008;112:13958.
21. Kyriacou SV, Brownlow WJ, Xu XHN. Biochemistry 2004;43:140. [PubMed: 14705939]
22. Xu XHN, Brownlow WJ, Kyriacou SV, Wan Q, Viola JJ. Biochemistry 2004;43:10400. [PubMed: 15301539]
23. Xu XHN, Chen J, Jeffers RB, Kyriacou SV. Nano Letters 2002;2:175.
24. X-HN, Xu; Patel, RP. Nanoparticles for Live Cell Dynamics. Nalwa, HS., editor. 2004.
25. Jain PK, Lee KS, El-Sayed IH, El-Sayed MA. J Phys Chem B 2006;110:7238. [PubMed: 16599493]
26. Kelly KL, Coronado E, Zhao LL, Schatz GC. J Phys Chem B 2002;107:668.
27. Lee KJ, Browning LM, Huang T, Ding F, Nallathamby PD, Xu X-HN. Anal Bioanal Chem. 201010.1007/s00216
28. Sonnichsen C, Reinhard BM, Liphardt J, Alivisatos AP. Nat Biotechnol 2005;23:741. [PubMed: 15908940]
29. Tabor C, Murali R, Mahmoud M, El-Sayed MA. J Phys Chem A 2009;113:1964.
30. Browning LM, Lee KJ, Huang T, Nallathamby PD, Lowman J, Xu XHN. Nanoscale 2009;1:138. [PubMed: 20644873]
31. Kyriacou SV, Nowak ME, Brownlow WJ, Xu XHN. J Biomed Opt 2002;7:576. [PubMed: 12421124]
32. Xu XHN, Brownlow WJ, Huang S, Chen J. Biochem Biophys Res Commun 2003;305:79. [PubMed: 12732199]

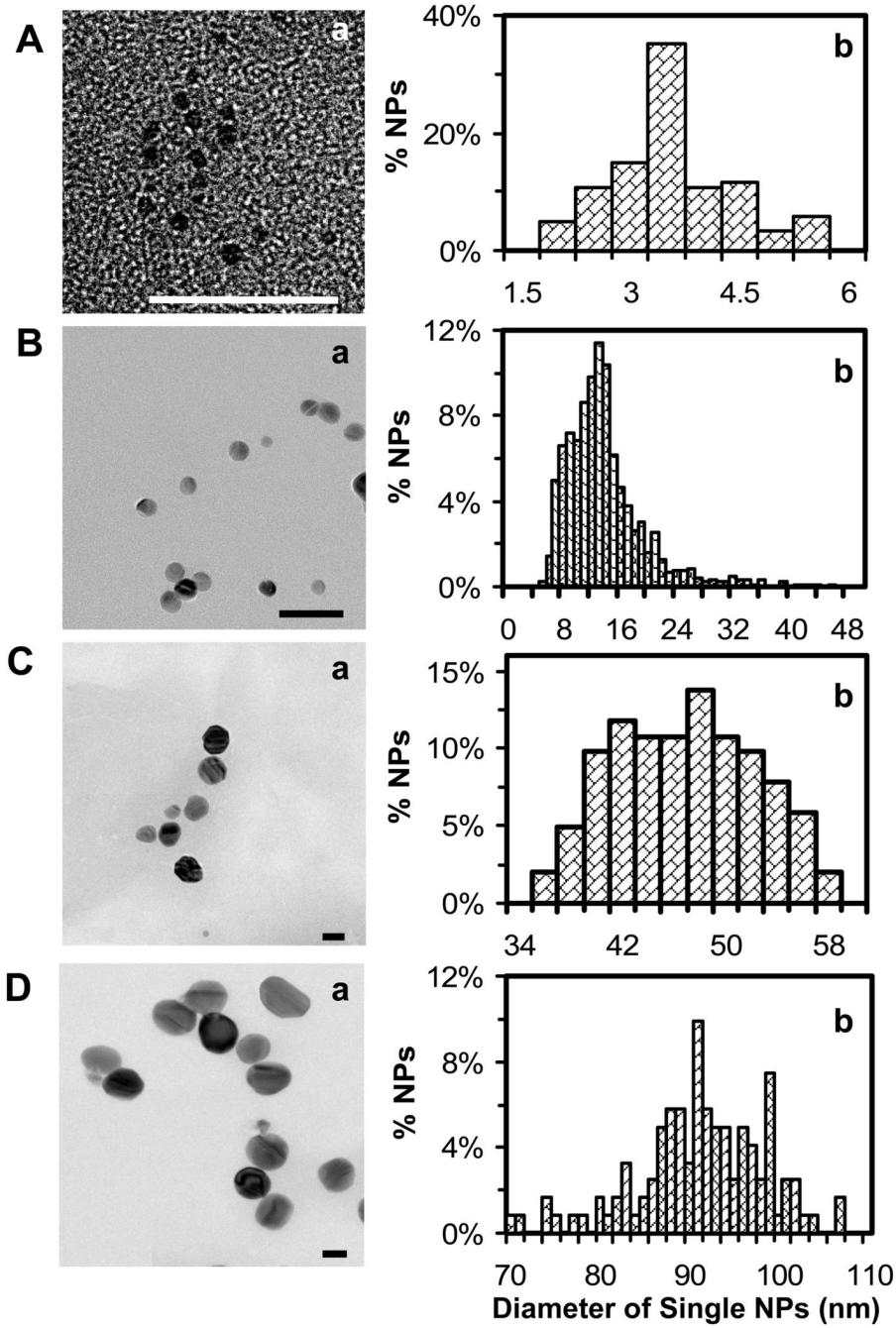

Figure 1.

Characterization of sizes and shapes of single Ag NPs using HRTEM: (a) representative HRTEM images and (b) histograms of distribution of diameters of single Ag NPs show nearly spherical shape single NPs with the average diameters of (A) 3.1 ± 0.6 nm, ranging 1.7–6 nm; (B) 13.4 ± 5.8 nm, ranging 5–45 nm; (C) 46.4 ± 6.1 nm, ranging 35–66 nm; and (D) 91.1 ± 7.6 nm, ranging 70–110 nm. For each sample, a minimal of 100 NPs was analyzed from 20 images, similar to the ones in (a). The scale bars are 25 nm in (A–B) and 50 nm in (C–D).

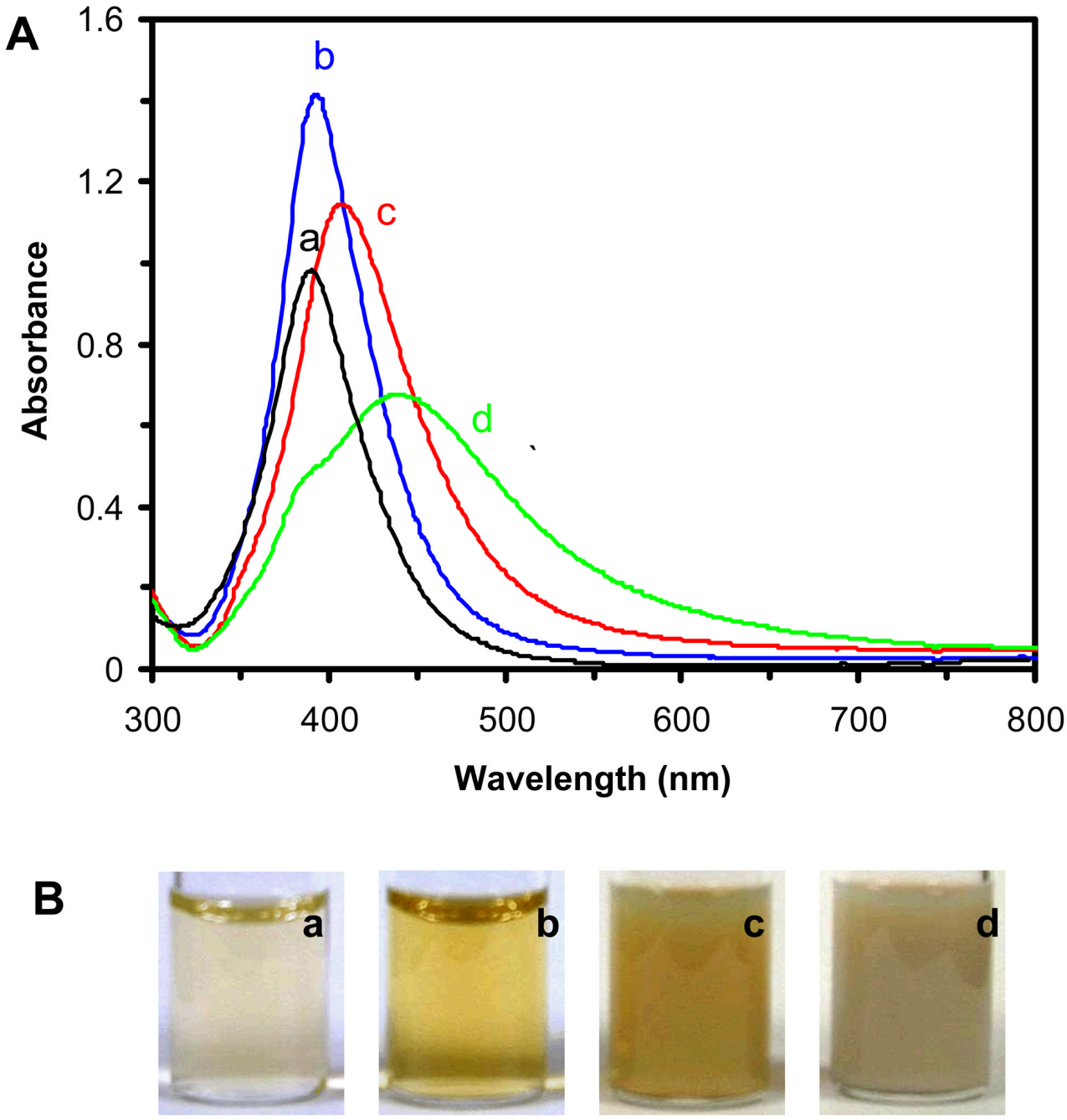

Figure 2.

Study of surface plasmon absorption and scattering of Ag NPs in bulk solution using UV-vis absorption spectroscopy:

(A) UV-vis absorption spectra of Ag NP solutions: (a) 30 nM of (3.1 ± 0.6) nm Ag NPs; (b) 0.7 nM of (13.4 ± 5.8) nm Ag NPs; (c) 0.2 nM of (46.4 ± 6.1) nm Ag NPs; and (d) 0.2 nM of (91.1 ± 7.6) nm Ag NPs, show the absorbance at peak-wavelength with FWHM: (a) 0.91 at 390 nm (FWHM = 62 nm); (b) 1.1 at 393 nm (FWHM = 65 nm); (c) 1.35 at 408 nm (FWHM = 82 nm); and (d) shoulder peak of 0.42 at 384 nm and primary peak of 0.63 at 440 nm (FWHM = 152 nm), respectively.

(B) Photos of the Ag NP solutions in (A).

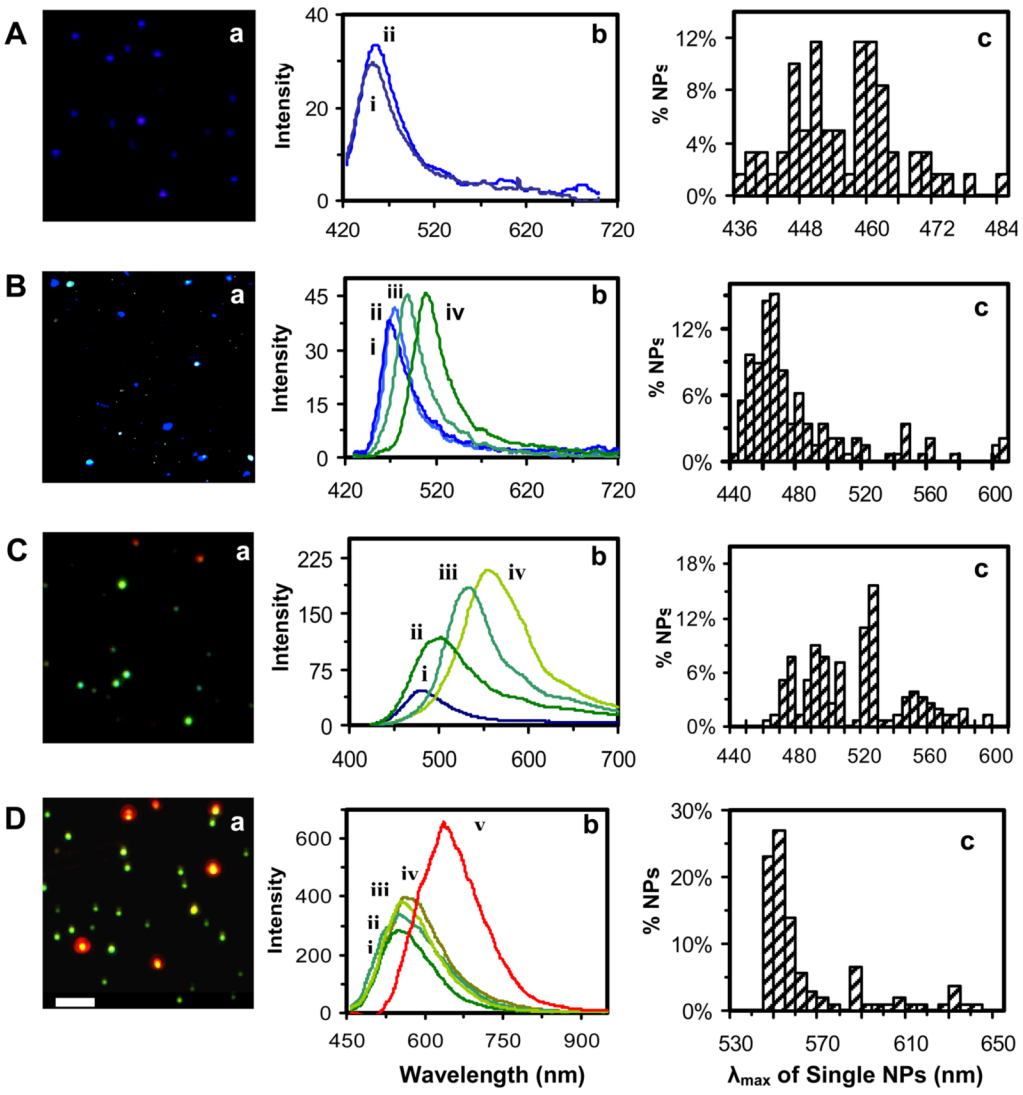

Figure 3.

Characterization of size-dependent LSPR spectra of single Ag NPs in solution: (a) representative dark-field optical color images of single Ag NPs, (b) representative LSPR spectra of single Ag NPs, and (c) histograms of the distribution of peak wavelength (λ_{max}) of LSPR spectra of single NPs, for (A) 3.1 ± 0.6, (B) 3.4 ± 5.8, (C) 46.4 ± 6.1, and (D) 1.1 ± 7.6 nm Ag NP solution, respectively. More than 300 of single NPs are studied for each solution to construct the histograms in (c). Scale bar of 2 μm in (a) shows the distances among single NPs, but not the sizes of NPs, because NPs are imaged under optical diffraction limit (~ 250 nm).

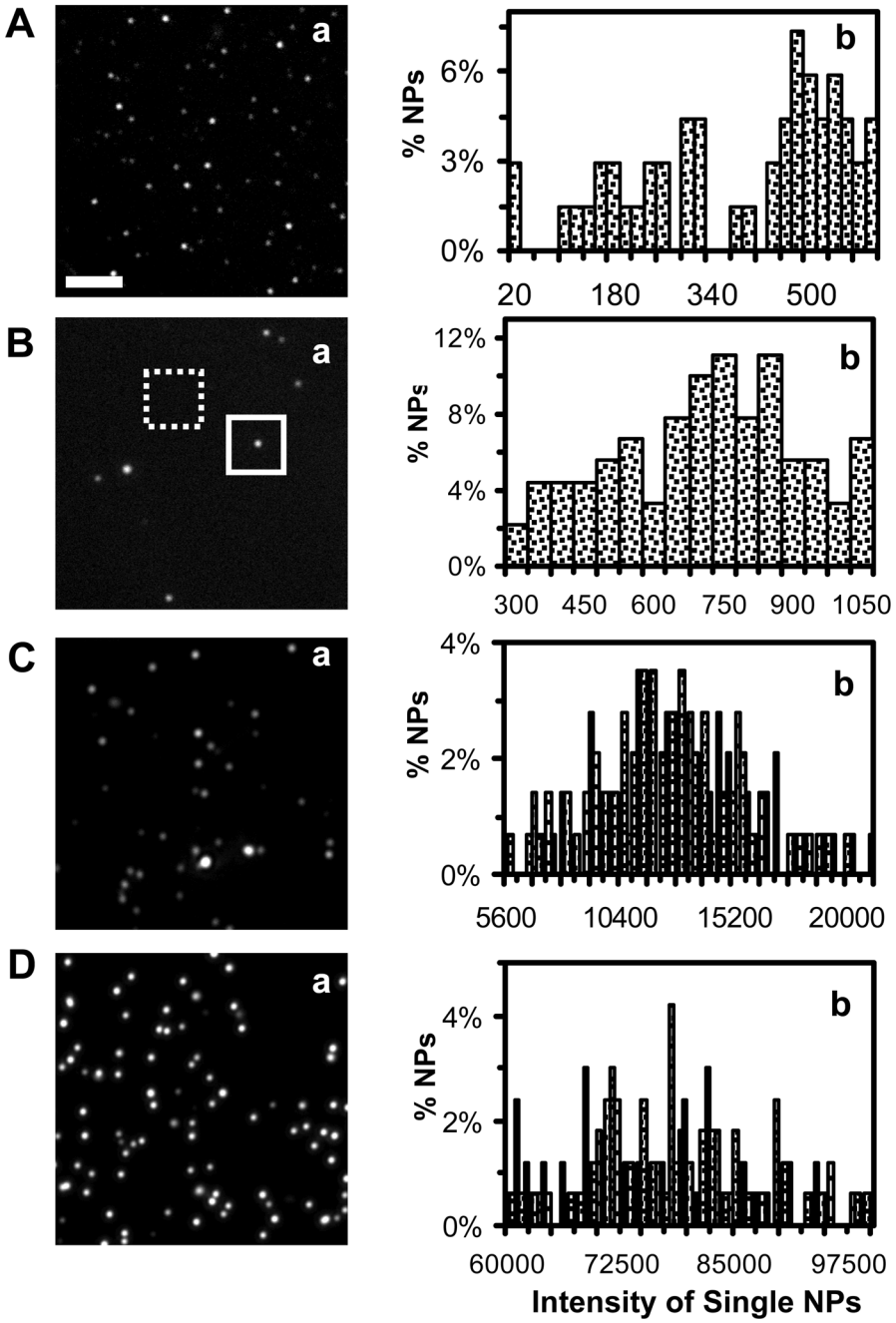

Figure 4.

Characterization of the size-dependent scattering intensity of single Ag NPs in solution: (a) representative dark-field optical images of single Ag NPs and (b) histograms of the distribution of scattering intensity of single NPs, for (A) 3.1 ± 0.6, (B) 13.4 ± 5.8, (C) 46.4 ± 6.1, and (D) 91.1 ± 7.6 nm Ag NP solution, respectively. More than 300 of single NPs were studied for each histogram in (b). The intensity scale of the optical images in (a) is (A) 88–134, (B) 70–160, (C) 80–400, and (D) 80–900 ADC, respectively. The scattering intensity of individual NPs is calculated by subtracting the average background intensity of individual background areas (20x20 pixel) in the absence of NPs, as outlined by a dashed-line square in (B), from the integrated intensity of a single NP in the same-sized detection area (20x20 pixel), as squared

in (B). Scale bar of 2 μm in (a) shows the distances among single NPs, but not the sizes of NPs, due to the optical diffraction limit (~ 250 nm).

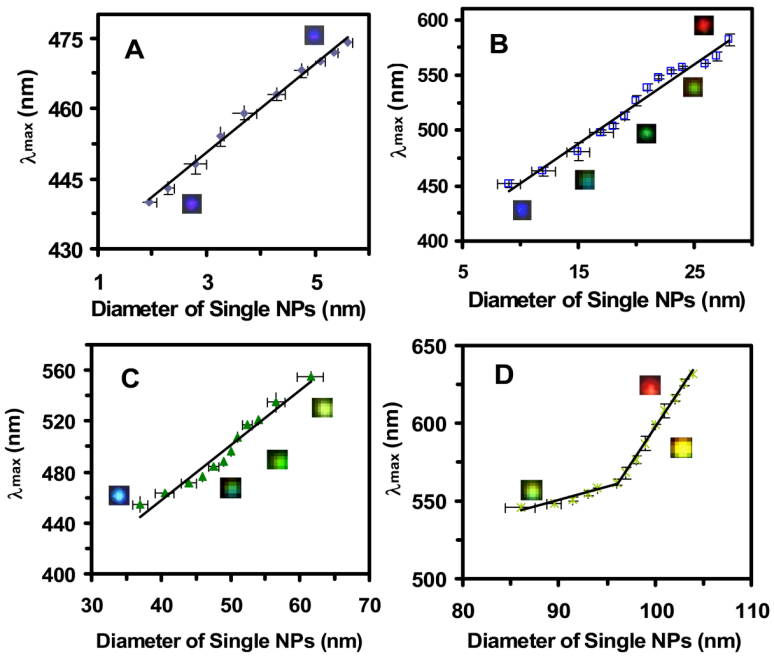

Figure 5.

Correlation of histograms of the distribution of λ_{max} of LSPR spectra of single Ag NPs with histograms of the distribution of the sizes of single NPs to create optical nano rulers. Plots of distribution of λ_{max} of LSPR spectra of single NPs (Figure 3c) versus their size distribution (Figure 1b) show size-dependent λ_{max} of single NPs, for individual NP solution: (A) 3.1 ± 0.6, (B) 13.4 ± 5.8, (C) 46.4 ± 6.1, and (D) 91.1 ± 7.6 nm Ag NPs, respectively. Selected single NP optical images are embedded in the plots. More than 300 of single NPs were studied for each plot. The points with error bars represent the averages of experimental measurements with their standard deviations and the lines are fitted to the experimental results using least-squares linear regression. The linear regressions for (A–D) are 0.99, 0.98, 0.96, 0.92 and 1.0, respectively.

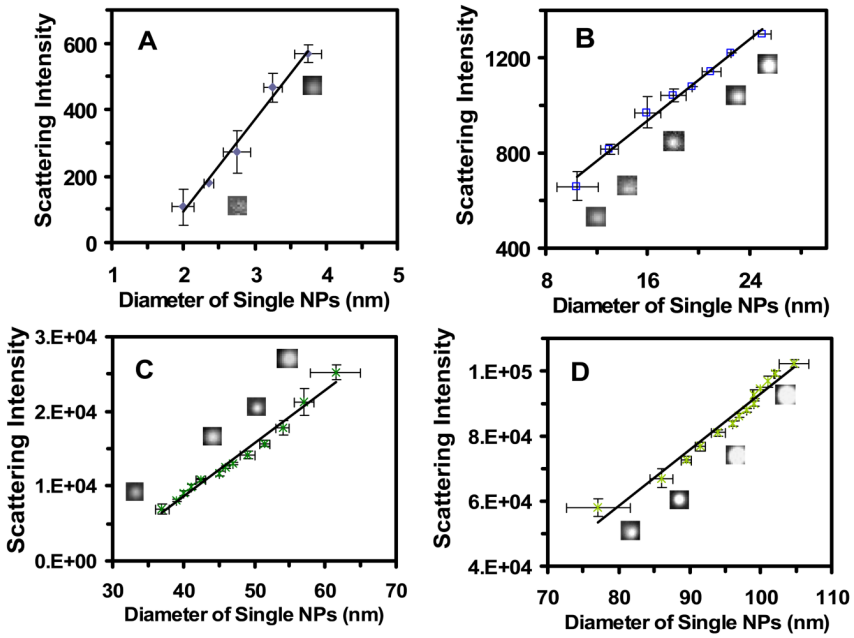

Figure 6.

Correlation of histograms of the distribution of scattering intensity of single Ag NPs with histograms of the distribution of the sizes of single NPs to create optical nano rulers. Plots of distribution of scattering intensity of single NPs (Figure 4b) versus their size distribution (Figure 1b) illustrate size-dependent scattering intensity of single NPs, for individual NP solution: (A) 3.1 ± 0.6, (B) 13.4 ± 5.8, (C) 46.4 ± 6.1, and (D) 91.1 ± 7.6 nm Ag NPs, respectively. Selected single NP optical images are embedded in the plots. More than 300 of single NPs were studied for each plot. The averages of experimental measurements with their standard deviations are shown in the points with error bars, and the lines represent the fitting of least-squares linear regression. The linear regressions for (A–D) are 0.99, 0.99, 0.98, and 0.97, respectively.

Table 1

Summary of Optical Nano Rulers (Calibration Curves) of Single NPs

Average Diameter (nm)	Diameter Range (nm)	λ_{max} Range[a] (nm)	Intensity Range [b] (ADC)	Linear Regression (R^2) [c]	
				λ_{max} vs size	Intensity vs size
3.1 ± 0.6	1.7–6	440–478	108 – 640	0.99	0.99
13.4 ± 5.8	5–45	452–594	$(0.66 – 1.32)\times10^2$	0.98	0.99
46.4 ± 6.1	35–66	455–555	$(0.69–2.52)\times10^3$	0.96	0.98
91.1 ± 7.6	70–96	544–562	$(0.58 – 1.02)\times10^5$	0.92	0.97
	97–110	568–662		1.0	

[a] Range of peak wavelength of single NPs in each solution.

[b] Range of scattering intensity of single NPs in each solution.

[c] Theoretic fitting of calibration curves with averages of experimental measurements of peak wavelength (λ_{max}) or scattering intensity of single NPs in each solution using least-squares method.